

J/ψ production in proton-lead collisions at LHCb

Fanfan JING^{*†}

Tsinghua University

E-mail: fanfan.jing@cern.ch

The production of prompt J/ψ and J/ψ from b -hadron decays has been studied in proton-lead collisions with the LHCb detector at the proton-nucleon centre-of-mass energy $\sqrt{s_{NN}} = 5$ TeV. The nuclear modification factor and forward-backward production ratio for prompt J/ψ are determined for the first time. The results show clear suppression of the J/ψ yield with respect to pp collisions in the forward region. Theoretical predictions are in good agreement with the experiment results. The analysis is based on a data sample corresponding to an integrated luminosity of 1 nb^{-1} .

The European Physical Society Conference on High Energy Physics

18-24 July, 2013

Stockholm, Sweden

^{*}Speaker.

[†]On behalf of the LHCb collaboration.

1 **1. Introduction**

2 Quarkonium production suppression is one of the most distinctive signatures of the formation
 3 of quark-gluon plasma (QGP) [1]. However, in heavy-ion collisions cold nuclear matter effect
 4 can also lead to the suppression of quarkonium [2–4]. Proton-nucleus (pA) collisions, where a
 5 QGP is not expected be created, provide a good platform to study cold nuclear matter effects [3].
 6 The nuclear modification factor $R_{pA} \equiv \sigma_{pA}/(A \times \sigma_{pp})$ and the forward-backward production ratio
 7 $R_{FB} \equiv R_{pA}^{\text{forward}}/R_{pA}^{\text{backward}}$ discussed below provide a quantitative measure for cold nuclear matter
 8 effects, where A is the atomic mass number of the nucleus [4].

9 The asymmetric layout of the LHCb experiment [5] allows a measurement of R_{pA} for both the
 10 forward (pA) and backward (Ap) regions, taking advantage of the inversion of the proton and lead
 11 beams during the pPb data-taking. The centre-of-mass energy of the proton-nucleon system is 5 TeV.
 12 Due to the asymmetry in the energy per nucleon in the two beams, the proton-nucleon centre-of-mass
 13 system has a rapidity in the laboratory frame of $+0.47$ (-0.47) for pA (Ap) collisions. Therefore,
 14 the rapidity range $1.5 < y < 4.0$ is studied for pA collisions, and $-5.0 < y < -2.5$ for Ap collisions.

15 This analysis is based on a data sample acquired during the pPb run in early 2013, corresponding
 16 to an integrated luminosity of 0.75 nb^{-1} (0.30 nb^{-1}) for pA (Ap) collisions. In this analysis the
 17 differential production cross-sections of prompt J/ψ and J/ψ from b -hadron decays are measured.
 18 The measurements of R_{pA} and R_{FB} for prompt J/ψ are presented. The results are preliminary and
 19 based on Ref. [6].

20 **2. Event selection and cross-section determination**

21 The J/ψ production cross-section measurement follows the approach described in Refs. [7–9].
 22 The J/ψ candidates are reconstructed and selected using dimuon final states. The candidates are
 23 selected from pairs of oppositely charged particles with transverse momentum $p_T > 0.7 \text{ GeV}/c$,
 24 which are identified as muons by the muon detector and have a track fit χ^2 per degree of freedom
 25 less than 3. The difference between the logarithms of the likelihoods for the muon and the pion
 26 hypotheses $DLL_{\mu\pi}$ [10] is required to be greater than 1.0. The two muons are required to originate
 27 from a common vertex with a χ^2 -probability larger than 0.5%. Candidates are kept if the invariant
 28 mass falls in a mass window of $\pm 120 \text{ MeV}/c^2$ around the known J/ψ mass [11].

29 The numbers of prompt J/ψ and J/ψ from b -hadron decays in bins of the kinematic variables
 30 y and/or p_T are obtained by performing a combined fit to the distributions of the dimuon invariant
 31 mass and the pseudo-proper time t_z in each kinematic bin. The pseudo-proper time of the J/ψ
 32 meson is defined as $t_z = \frac{\Delta z \times M_{J/\psi}}{p_z}$, where Δz is the distance along the beam axis z between the J/ψ
 33 decay vertex and its associated primary vertex refitted after removing the two muon tracks from the
 34 J/ψ candidate, p_z the measured J/ψ momentum in z direction, and $M_{J/\psi}$ the known J/ψ mass [11].

35 The signal dimuon invariant mass distribution in each p_T and y bin is modelled by a Crystal
 36 Ball (CB) function [12], and the combinatorial background by an exponential function. The t_z
 37 signal distribution is described by the sum of a delta function at $t_z = 0$ for the prompt J/ψ and an
 38 exponential decay function for the J/ψ from b component, convolved with a resolution function
 39 modelled by a double-Gaussian function. The t_z background distribution in each kinematic bin
 40 is independently modelled with an empirical function based on the t_z distribution of background

41 using the *sPlot* technique [13]. The total fit function is the sum of the products of the mass and t_z fit
 42 functions for the signal and background components. Figure 1 shows projections of the fit on mass
 43 and t_z . The resolutions of the dimuon invariant mass in pA and Ap samples are consistent with each
 other, about $15 \text{ MeV}/c^2$, and are both consistent with that in pp collisions. The yields of prompt

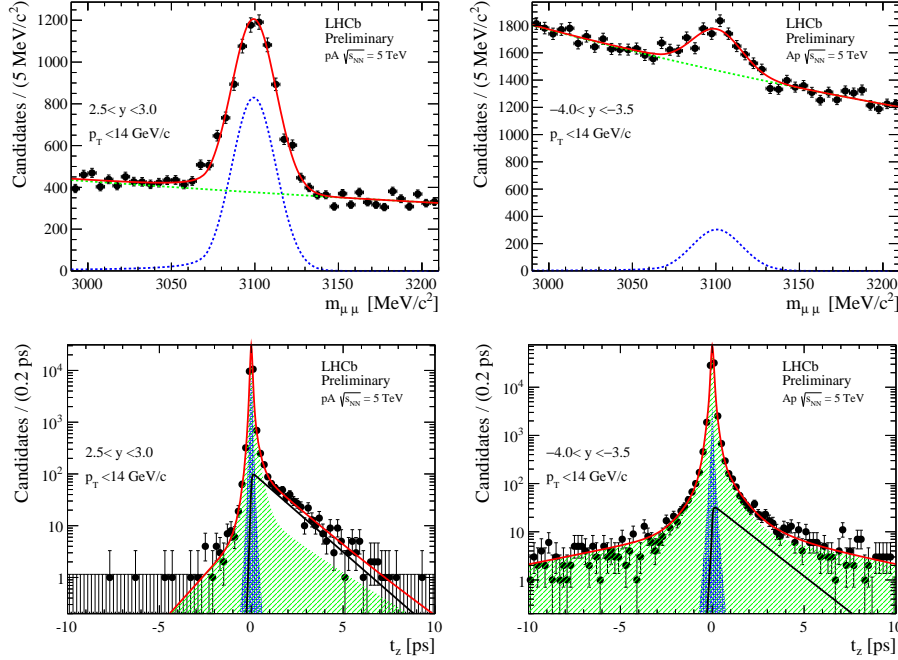


Figure 1: Projections of the combined fit onto (top) invariant dimuon mass and (bottom) t_z in pA (left) and Ap (right) samples. For the mass projection the total fitted function is shown (red solid line) together with the signal distribution (blue dotted line) and background (green dotted line). For the t_z projection the total fitted function is shown by the solid red line, the background indicated by the green hatched area, the prompt signal by the blue area and J/ψ from b by the solid black line.

44 J/ψ and J/ψ from b are then corrected with the efficiency event-by-event. The efficiency depends
 45 on p_T and y , and includes the geometrical acceptance, reconstruction and trigger efficiencies. The
 46 acceptance and reconstruction efficiencies are estimated from the simulated samples. The trigger
 47 efficiency is obtained from the data by exploiting a sample of J/ψ events that would still be triggered
 48 if the J/ψ candidates were removed. The differential cross-section is defined as the efficiency
 49 corrected number of J/ψ signal candidates in the given bin divided by the integrated luminosity, the
 50 branching fraction of the $J/\psi \rightarrow \mu^+ \mu^-$ decay, and the widths of the p_T and y bins.
 51

52 3. Systematic uncertainties

53 The different contributions to the systematic uncertainties affecting the cross-section measure-
 54 ment are discussed in the following and summarised in Table 1. The influence of the fit function
 55 used to describe the shape of the dimuon invariant mass distribution is estimated by fitting the
 56 invariant mass distribution with the sum of two Crystal Ball functions. The uncertainty of the
 57 luminosity determination is estimated to be 5% according to earlier studies [14]. The uncertainty
 58 due to reconstruction efficiency of the muon tracks is estimated using a data-driven tag-and-probe

Table 1: Relative systematic uncertainties on the differential production cross-section.

Source	Systematic uncertainty (%)
<i>Correlated between bins</i>	
Mass fits	1.8
Tracking efficiency	1.5
$\mathcal{B}(J/\psi \rightarrow \mu^+ \mu^-)$	1.0
Luminosity	5.0
t_z fit (only for <i>J/ψ</i> from <i>b</i>)	5.0
Vertexing, track quality, etc.	3.5
<i>Uncorrelated between bins</i>	
Binning	0.1 to 14

59 approach [15] based on partially reconstructed *J/ψ* decays. The uncertainties related to the radiative
60 tail, vertexing, track quality and muon identification are taken from Refs. [7–9], but have been
61 increased conservatively by 30%, leading to an overall uncertainty of 3.5%. The same has been
62 done for the uncertainty due to the t_z fit procedure, which only affects the component of *J/ψ* from *b*.
63 An uncertainty of 5% has been conservatively assigned. Differences in the p_T and y spectra between
64 the data and MC can effect the result because of the finite size of the bins. To estimate this affect,
65 the total efficiency has been checked by doubling the number of bins in p_T and rapidity. The relative
66 difference with respect to the nominal binning, is taken as systematic uncertainty.

67 4. Results

68 The single differential cross-sections for prompt *J/ψ* production and *J/ψ* from *b* in *pA* and
69 *Ap* as functions of p_T and y , assuming no *J/ψ* polarization, are shown in Fig. 2. The integrated
70 cross-section for prompt *J/ψ* with $p_T < 14 \text{ GeV}/c$ in *pA* ($1.5 < y < 4.0$) and *Ap* ($-5.0 < y < -2.5$)
71 regions is $\sigma_{pA} = 1028 \pm 14_{(\text{stat.})} \pm 89_{(\text{syst.})} \mu\text{b}$, $\sigma_{Ap} = 1142 \pm 50_{(\text{stat.})} \pm 98_{(\text{syst.})} \mu\text{b}$; that for *J/ψ* from
72 *b* is $\sigma_{pA} = 150 \pm 4_{(\text{stat.})} \pm 13_{(\text{syst.})} \mu\text{b}$, $\sigma_{Ap} = 120 \pm 8_{(\text{stat.})} \pm 10_{(\text{syst.})} \mu\text{b}$.

73 The *J/ψ* production cross-section in *pp* collisions at 5 TeV used as a reference to determine
74 the nuclear modification factor R_{pA} is obtained by a linear interpolation from previous LHCb
75 measurements [7–9] within $p_T < 14 \text{ GeV}/c$ and $2.5 < y < 4.0$. In the left plot of Fig. 3, the nuclear
76 modification factor R_{pA} as a function of y compared to the theoretical predictions is shown. The
77 forward-backward production ratio R_{FB} , which does not rely on the reference cross-section in *pp*
78 collisions, is shown in the right plot of Fig. 3.

79 5. Update of the analysis

80 The analysis has been updated since the EPS 2013 conference, and the paper has already been
81 submitted to JHEP [16]. The final results are based on a data sample corresponding to an integrated
82 luminosity of 1.1 nb^{-1} (0.5 nb^{-1}) for forward (backward) collisions. The nuclear modification
83 factor and forward-backward production ratio as a function of y are determined not only for prompt

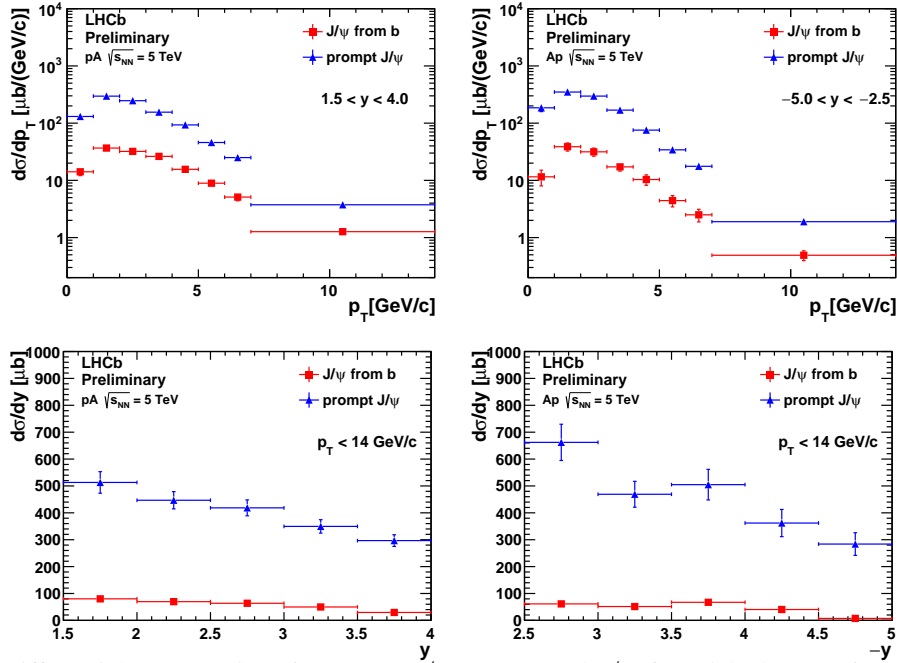


Figure 2: Differential cross-sections for prompt J/ψ mesons and J/ψ from b -hadrons as functions of (top) p_T and (bottom) y in (left) forward and (right) backward regions.

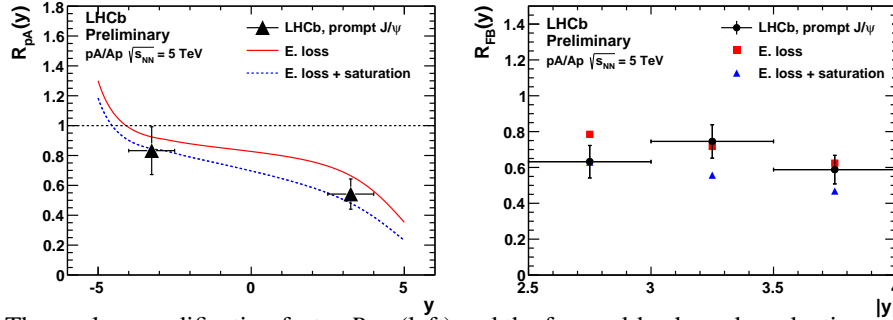


Figure 3: The nuclear modification factor $R_{pA}(y)$ (left) and the forward-backward production ratio $R_{FB}(y)$ (right) as a function of y . The measurements agree well with the theoretical predictions [4].

84 J/ψ but also for J/ψ from b . The forward-backward production ratio is also measured as a function
 85 of p_T . Figure 4 shows the final result for the nuclear modification factor as a function of y .

86 **6. Conclusion**

87 The production of J/ψ mesons with rapidity $1.5 < y < 4.0$ (pA) and $-5.0 < y < -2.5$ (Ap), and
 88 transverse momentum $p_T < 14$ GeV/ c , is studied with the LHCb detector in proton-lead collisions
 89 at the proton-nucleon centre-of-mass energy $\sqrt{s_{NN}} = 5$ TeV. The nuclear modification factor R_{pA}
 90 and the forward-backward asymmetry ratio R_{FB} are determined as a function of y . The results show
 91 clear cold nuclear matter effects, and are in good agreement with the theoretical predictions.

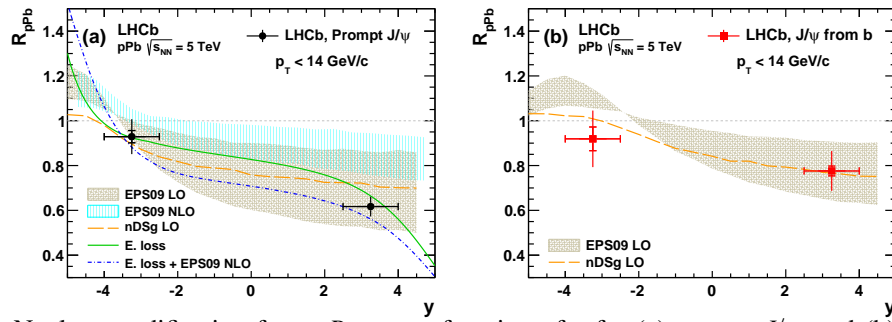


Figure 4: Nuclear modification factor R_{pPb} as a function of y for (a) prompt J/ψ and (b) J/ψ from b , compared with the theoretical predictions [2–4].

92 References

- 93 [1] T. Matsui and H. Satz, J/ψ suppression by quark-gluon plasma formation, *Phys.Lett.* **B178** (1986) 416.
- 94 [2] E. G. Ferreira, F. Fleuret, J. P. Lansberg, and A. Rakotozafindrabe, *Impact of the nuclear modification of*
- 95 *the gluon densities on J/ψ production in pPb collisions at $\sqrt{s_{NN}} = 5$ TeV*, arXiv:1305.4569.
- 96 [3] J. Albacete, N. Armesto, R. Baier, G. G. Barnafoldi, J. Barrette, *et al.*, *Predictions for p+Pb collisions*
- 97 *at $\sqrt{s_{NN}} = 5$ TeV*, *Int. J. Mod. Phys.* **E22** (2013) 1330007 [arXiv:1301.3395].
- 98 [4] F. Arleo and S. Peigne, *Heavy-quarkonium suppression in p-A collisions from parton energy loss in*
- 99 *cold QCD matter*, *JHEP* **03** (2013) 122 [arXiv:1212.0434].
- 100 [5] LHCb collaboration, A. A. Alves Jr. *et al.*, *The LHCb detector at the LHC*, *JINST* **3** (2008) S08005.
- 101 [6] LHCb collaboration, *Study of the J/ψ production cross-section in proton-lead collisions at*
- 102 *$\sqrt{s_{NN}} = 5$ TeV*, May, 2013.
- 103 [7] LHCb collaboration, R. Aaij *et al.*, *Measurement of J/ψ production in pp collisions at $\sqrt{s} = 7$ TeV*,
- 104 *Eur. Phys. J.* **C71** (2011) 1645 [arXiv:1103.0423].
- 105 [8] LHCb collaboration, R. Aaij *et al.*, *Measurement of J/ψ production in pp collisions at $\sqrt{s} = 2.76$ TeV*,
- 106 *JHEP* **02** (2013) 41 [arXiv:1212.1045].
- 107 [9] LHCb collaboration, R. Aaij *et al.*, *Production of J/ψ and Υ mesons at $\sqrt{s} = 8$ TeV*, *JHEP* **06** (2013)
- 108 64 [arXiv:1304.6977].
- 109 [10] F. Archilli *et al.*, *Performance of the muon identification at LHCb*, arXiv:1306.0249. submitted to
- 110 JINST.
- 111 [11] Particle Data Group, J. Beringer *et al.*, *Review of particle physics*, *Phys. Rev.* **D86** (2012) 010001. and
- 112 2013 partial update for the 2014 edition.
- 113 [12] T. Skwarnicki, *A study of the radiative cascade transitions between the Upsilon-prime and Upsilon*
- 114 *resonances*. PhD thesis, Institute of Nuclear Physics, Krakow, 1986. DESY-F31-86-02.
- 115 [13] M. Pivk and F. R. Le Diberder, *sPlot: a statistical tool to unfold data distributions*, *Nucl.Instrum.Meth.*
- 116 **A555** (2005) 356–369 [arXiv:physics/0402083].
- 117 [14] LHCb collaboration, *First look at the pPb pilot run*, Jan, 2013.
- 118 [15] A. Jaeger, P. Seyfert, M. De Cian, J. van Tilburg, and S. Hansmann-Menzemer, *Measurement of the*
- 119 *track finding efficiency*, Apr, 2012.
- 120 [16] LHCb collaboration, R. Aaij *et al.*, *Study of J/ψ production and cold nuclear matter effects in pPb*
- 121 *collisions*, arXiv:1308.6729. submitted to JHEP.